JOURNAL OF GUIDANCE, CONTROL, AND DYNAMICS
Vol. 21, No. 6, November–December 1998

Experimental Evaluation of the Torque-Shaping Method for Slew Maneuver of Flexible Space Structures

Jinyoung Suk* and Youdan Kim†
Seoul National University, Seoul 151-742, Republic of Korea
and
Hyochoong Bang‡
Korea Aerospace Research Institute, Daejon 305-600, Republic of Korea

A torque-shaping method using trigonometric series expansion and optimization is demonstrated experimentally for a flexible space structure testbed. The hub–appendage structure is carefully designed and assembled to provide an environment to achieve the rest-to-rest maneuver and vibration suppression. The reaction wheel assembly is used as an actuator to drive the structure, while an encoder, a gyroscope, and a piezoelectric transducer are used as sensors to detect the slew/flexible motion. The experimental testbed is identified by applying an optimization technique using the data of the structure actuated by an impulsive hub control torque. With the well-adjusted experimental environment, the open-loop experiment results using the torque-shaping method match well with those of the numerical simulations. Furthermore, the closed-loop experiment results show that precise targeting is achieved in the presence of various external disturbances. The proposed method will provide an efficient basis for implementing a realizable torque-shaping strategy for the slewing of flexible space structures.

I. Introduction

RECENTLY there has been considerable interest in the time-optimal rest-to-rest maneuver for flexible spacecraft, without significant structural vibrations during and at the end of the maneuver.[1–6] The minimum time solution requires a bang-bang type control that may introduce unintended excitation to the high-frequency modes. To solve this problem, Liu and Wie[1] imposed constraints on flexible modes for no residual structural vibration after the maneuver to determine the optimal switching times. Singh and Vadali[2] solved a similar problem in the frequency domain by introducing the time-delay filter concept. Singhose et al.[3] presented a robust input shaping method for limiting deflection during the slew. Note that all of these torque-shaping techniques use on–off command signals. Another approach is to design a control torque that exhibits a high degree of smoothness, to avoid exciting the high-frequency dynamics of a flexible system. Junkins et al.[4] introduced a near-minimum-time tracking law based on Lyapunov stability theory, and Aspinwall[5] and Suk et al.[6] proposed various torque-shaping methods in the frequency region.

This paper puts the utmost emphasis on the experimental demonstrations of the torque-shaping methods and closed-loop tracking control suggested in Ref. 6. The proposed open-loop control method is to achieve a large-angle slewing in view of the vibration suppression and minimization of maneuver time. Therefore, it would be appropriate to mention that the developed control method can provide good and realizable performance beyond the region of a pure desk plan by applying the open-loop/closed-loop control laws to the flexible space structure testbed at Seoul National University (FSST/SNU). FSST/SNU is somewhat similar to the U.S. Air Force Office of Scientific Research at Texas A&M University facility,[4] except that FSST/SNU uses a pizoelectric sensor instead of strain gauges to determine the bending moment of the appendage. FSST/SNU also uses a piezoelectric vibrating type gyroscope in addition to the encoder measuring the angular information. FSST/SNU is composed of a central hub and four identical appendages to allow single axis slew maneuvers. A reaction wheel type actuator is mounted on the hub, which consists of a torque motor and a wheel assembly. An encoder and a gyroscope are used to measure the hub angle and hub angular velocity, and a piezoelectric sensor is attached to the root of one of the appendages to measure the flexible mode.

This paper is organized as follows. First, a brief review of the optimal torque-shaping method is presented. A detailed description of the FSST/SNU hardware is provided. System identification is performed to revise the mathematical model to obtain the realistic dynamic characteristics. The open-loop experimental results are compared with the numerical simulation, and the proposed torque-shaping method is compared with the two competitive alternatives: 1) bang-bang control and 2) near-minimum-time maneuver control. Finally, the Lyapunov tracking (closed-loop) controller is realized to achieve accurate targeting in the presence of the presumed environmental disturbances.

II. Open-Loop Optimal Torque Shaping

In this section, a brief review of the optimal torque-shaping method is presented for the slew maneuver of the FSST/SNU shown in Fig. 1. Configuration parameters of the FSST/SNU are listed in Table 1. After the equation of motion is derived in modal coordinates, the performance index is assigned to extract the optimally shaped control torque. Analytic expressions of the performance index and its derivatives are used to enhance the optimization algorithm in terms of numerical accuracy.

A. Mathematical Model of FSST/SNU

Consider the planar rotational/vibrational dynamics of a flexible structure consisting of rigid and antisymmetric structural modes. The governing equation of motion is obtained using a finite element method[7]

$$\boldsymbol{M}\ddot{\boldsymbol{x}} + \boldsymbol{K}\boldsymbol{x} = \boldsymbol{F}u_r \tag{1}$$

where

$$\boldsymbol{M} = \begin{bmatrix} J_h + 4M_{\theta\theta} & 4M_{\theta v} \\ 4M_{\theta v}^T & 4M_{vv} \end{bmatrix}, \quad \boldsymbol{K} = \begin{bmatrix} 0 & \boldsymbol{0}_{1\times 2n}^T \\ \boldsymbol{0}_{1\times 2n} & 4K_{vv} \end{bmatrix}, \quad \boldsymbol{F} = \begin{bmatrix} 1 \\ 0 \\ 0 \\ \vdots \end{bmatrix} \tag{2}$$

Received Feb. 6, 1998; revision received June 15, 1998; accepted for publication July 4, 1998.

*Graduate Student, Department of Aerospace Engineering; currently Research Engineer, Aerospace Defense Division, Daewoo Heavy Industries, Ltd., Changwon 641-120, Republic of Korea. Member AIAA.
†Associate Professor, Department of Aerospace Engineering. Senior Member AIAA.
‡Research Scientist, Koreasat Group/Space Division. Member AIAA.

Table 1 Configuration parameters of FSST/SNU

Parameter	Value
Radius of hub, m	0.20
Rotary inertia of hub, kg/m^3	0.8971
Mass density of appendage, kg/m^3	2800
Young's modulus of appendage, N/m	7.5842×10^{10}
Thickness of appendage, m	0.0020
Width of appendage, m	0.0635
Length of appendage, m	0.8100

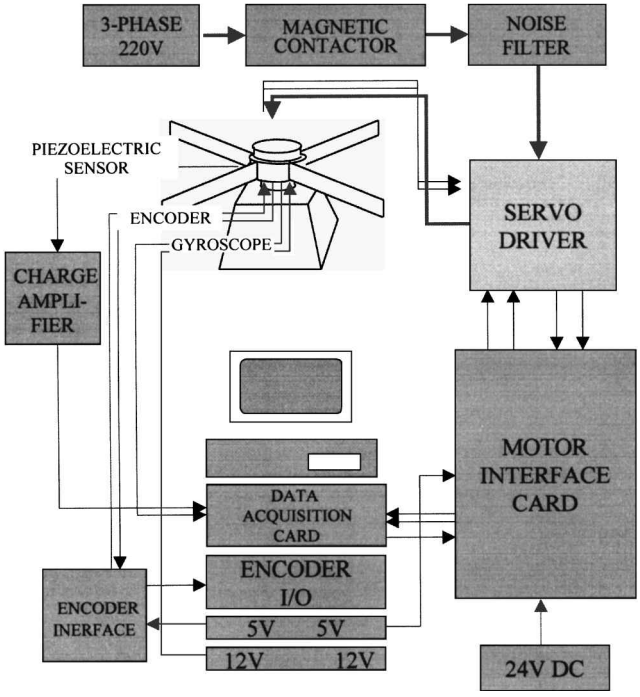

Fig. 1 Integrated structure–control signal flow diagram.

$$M_{\theta\theta} = \int_{l_0}^{l} \rho x^2 \, \mathrm{d}x, \qquad M_{\theta v} = \sum_i \int_{l_0}^{l} \rho x \phi_i(x) \, \mathrm{d}x$$

where l_0 is radius of the hub, l is the distance from the center of hub to the tip of the appendage, $M_{\theta v}$ is a coupling matrix between rigid and structural modes, and M_{vv} and K_{vv} denote mass and stiffness matrices of flexible mode, respectively. The states are composed of the rigid mode and flexible dynamics of elastic modes as follows:

$$\boldsymbol{x} = [\Theta \quad w_1 \quad \theta_1 \quad w_2 \quad \theta_2 \quad \cdots \quad w_i \quad \theta_i \quad \cdots]^T \tag{3}$$

where Θ, w_i, and θ_i denote the hub angle, bending displacement, and angle of the ith finite element node, and $\phi_i(x)$ denotes shape function, respectively.

B. Slewing Control Laws

1. Bang-Bang Maneuver

It is well known that the minimum time solution for a single-axis rest-to-rest maneuver takes the form of bang-bang control.[8] In this control method, constant torque is applied in positive direction for the first half and negative direction for the second half of the maneuver.

2. Near-Minimum-Time Maneuver

In the practical point of view, the reaction wheel assembly cannot generate ideal bang-bang torque profile. Even if the computer sends out the sharp signal, the mechanical/electrical time constant prevents the servodriver from generating an abrupt torque variation. Therefore, a realistic alternative is a modified torque command curve that splines the three discontinuities of the bang-bang history. The torque shape is divided into the five subdomains in near-minimum-time maneuver control, and the three discontinuous regions are smoothed using the cubic polynomials. Coefficients for the polynomials are determined to satisfy the conditions at each boundary of maneuver interval.[4]

3. Optimal Maneuver Using the Torque-Shaping Method

In a similar context to the previous near-minimum-time maneuver, Fourier series expansion can be used to reshape the bang-bang input so that the structural modes excitation may be minimized. Fourier series of the modified bang-bang torque input can be expressed as follows[6]:

$$u_r(t) = \sum_{i=1}^{N} a_i \sin \frac{2\pi i t}{t_f} \tag{4}$$

where

$$a_i = -\frac{2u_{\max}}{i\pi} \cos i\pi [1 - \cos(1-\delta) i\pi], \qquad u_{\max} = \frac{4 J_{\text{tot}} \Theta_f}{(1-\delta)^2 t_f^2}$$

The maneuver time t_f, the number of terms N of the trigonometric series, and the shaping parameter δ control the smoothness of the modified shaping torque and, therefore, the vibration energy of the system. In this study, target final angle is set to be 60 deg. To analyze the effect of Fourier series type input on the system dynamics, the modal coordinate expression is used. To perform the modal coordinate transform, we introduce the general modal coordinate transformation[7]

$$\boldsymbol{x} = \Phi \eta \tag{5}$$

where Φ is the modal matrix satisfying the biorthogonality conditions

$$\Phi^T \boldsymbol{M} \Phi = \boldsymbol{I}, \qquad \Phi^T \boldsymbol{K} \Phi = \operatorname{diag}\begin{pmatrix} \cdots & \omega_i^2 & \cdots \end{pmatrix} \equiv \Lambda$$

The transformed equation of motion becomes

$$\ddot{\eta}_j + \omega_j^2 \eta_j = \psi_j \sum_{i=1}^{N} a_i \sin \frac{2\pi i t}{t_f} \tag{6}$$

where ψ_j is the jth element of $\Phi^T \boldsymbol{F}$. From Eq. (6) it is obvious that the Fourier series input should avoid frequency components identical and/or close to those of modal coordinates to prevent possible resonance responses caused by the flexible appendages.

Equation (4) represents the input torque profile. For slewing and vibration suppression of the structure, the coefficients of trigonometric series in Eq. (4) are adopted as design variables to determine the input shape by an optimization procedure. A performance index can be defined in such a way that the vibration energy during maneuver and residual variation are minimized. The performance index in this study consists of three objective functions: 1) vibration energy of the appendage during maneuver, 2) vibration energy at the end of maneuver, and 3) the mean square error between the modified bang-bang input and reaction wheel torque to be optimized. First, the objective function $\boldsymbol{J}_1$ represents the vibration energy of the flexible structure during maneuver as follows:

$$\boldsymbol{J}_1 = \int_0^{t_f} \sum_{i=0}^{m} \left(\omega_i^2 \eta_i^2 + \dot{\eta}_i^2 \right) \mathrm{d}t \tag{7}$$

where η_0 denotes the modal coordinate of the rigid mode, η_i $(i = 1, 2, \ldots, m)$ denotes the modal coordinate of structural modes, and m is the number of flexible modes to be considered.

Objective function $\boldsymbol{J}_2$ represents the residual vibration energy at the end of maneuver:

$$\boldsymbol{J}_2 = \sum_{i=1}^{m} \left(\omega_i^2 \eta_i^2 + \dot{\eta}_i^2 \right) \Big|_{t_f} \tag{8}$$

To reduce the peak magnitude we adopt the objective function $\boldsymbol{J}_3$ that takes the mean square error between the modified bang-bang

input and reaction wheel torque to be optimized. It can be formulated as follows:

$$J_3 = \left[\frac{u_{\max}^2 (1-\delta) t_f}{2} + \frac{t_f}{4} \sum_{i=1}^{N} a_i^2 + \frac{u_{\max} t_f}{\pi} \sum_{i=1}^{N} \frac{a_i}{i} (\cos i\pi - \cos i\pi\delta) \right] \quad (9)$$

The performance index can be expressed as follows:

$$J = \sum_{i=1}^{3} \beta_i J_i$$

where β_i $(i = 1, 2, 3)$ is a weighting factor to balance the relative contribution of each objective function to the performance index. A separate study shows that the ratio between β_1 and β_2 mainly affects the residual vibration, whereas the results similar to those of the unconstrained optimization are obtained showing high peak magnitudes of the control torque as β_3 gets smaller.

Two constraints are imposed on the final target angle to guarantee the rest-to-rest maneuver. What is imposed on the final target angle can be expressed as follows:

$$J_{\text{tot}} \Theta_f = \sum_{i=1}^{N} \frac{a_i}{2\pi i} t_f^2 \quad (10)$$

where J_{tot} is the moment of inertia of the whole system. The other constraint that the angular velocity should be zero at the end of the maneuver is satisfied automatically once Eq. (10) is satisfied. Therefore the minimum requirement to achieve the rest-to-rest maneuver can be expressed by Eq. (10). Derivatives of the objective functions are required for applying a gradient-based optimization algorithm. The analytical expressions of performance index during the optimization process not only reduce computational time but also produce a better solution for optimization.[6] Once the coefficients are determined, the control torque can be calculated by a simple algebra. The control torque obtained herein is extremely smoothed so that it might be easy to implement.

III. Experimental Setup

A. Flexible Space Structure Testbed

FSST/SNU is composed of a central hub and four identical appendages. The hub is representative of the body of a spacecraft, and the appendages play the role of flexible solar panels. A reaction wheel assembly is used as an actuator to slew the hub–appendage structure. An encoder and a gyroscope mounted on the hub measure the slew angle and the angular velocity of the structure, respectively. A piezoelectric sensor is used to measure the flexible deformation that can be used to estimate the root bending moment of the appendage. The integrated structure-control signal flow is diagrammed in Fig. 1.

B. Vibration Analysis and Identification of FSST/SNU

In this section, vibration analysis of FSST/SNU is performed, and the mathematical model is modified to approximate the FSST/SNU. In the previous section, a mathematical model is obtained using a finite element method. The slew mode and the first three flexible modes are used for system identification. Natural frequencies of the mathematical model are coupled with their vibrating modes and can be extracted using the eigensystem analysis for the mass/stiffness matrices.

Figure 2 shows the frequency response of the FSST/SNU by an impulsive torque actuation. The first three natural frequencies including the rigid mode are measurable from the fast Fourier transform plot of the response. A vibrational mode test revealed modes at 3.11, 16.00, and 44.43 Hz. Measured natural frequencies are compared with the mathematical model in the right half side of Table 2, from which we can get the information on the system to be identified. From the results shown in Table 2, we can see that the mathematical model and the experimental model have similar frequency spectra. However, a more refined mathematical model can be obtained by minimizing the error between the measured and estimated frequency spectra, and this can improve the similarity between the measured and estimated output responses using the open-loop/closed-loop control laws.

Table 2 Natural frequencies and identified system parameters

Parameters	Initial value	Identified value	Mode[a]	Initial frequency, Hz	Identified frequency, Hz	Measured frequency, Hz
J_{tot}	0.8500	0.8971	2	3.19	3.11	3.11
ρ	0.3556	0.4139	3	16.66	16.00	16.00
EI	3.2106	3.4421	4	45.97	44.10	44.43

[a]The first mode is a rigid mode with a natural frequency of 0 Hz.

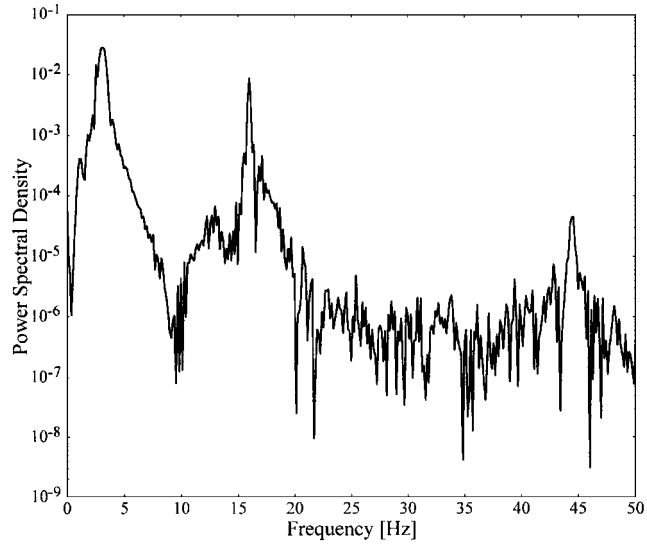

Fig. 2 Vibration mode test.

IV. Slew Maneuver Experiments

In this section, slew maneuvers with the suppression of the vibratory modes caused by the appendages are experimentally demonstrated to validate the effect of the designed optimal torque shaping and closed-loop control.

FSST/SNU is developed to implement optimal control laws for both large angle slewing and vibration control. For this purpose, the computed open-loop control torque is sent out to the servodriver by the main processor through the data acquisition system. The analog torque signal is discretized at each step to obtain the continuously varying output voltage and is assigned to the motor to move the hub to follow the desired trajectory. Especially, it is required to investigate the response of the structure to validate various physical/material properties and to compare the experimental results with those performed by the numerical simulation. Also note that well-performed open-loop results provide a good environment for the closed-loop implementation.

Friction is a main factor to be considered to obtain accurate open-loop responses of the system. Excellent optimal control trajectories often result in undesirable responses if the friction is not considered in the experiment. Note again that the friction affects in opposite direction during the overall region of the maneuver. This allows the evaluation of a new moment history where the effect of friction can be treated as a constant, vanishing in both the initial and the final state. In the experimental results to be shown hereafter, 25.5% of the designed torque was considered to overcome the effect of friction.

A. Open-Loop Control Experiment

In this study, open-loop experiments are performed, and the results are investigated in various aspects to show the systematic experimental methodology. First, the open-loop torque-shaping experiments are compared with the numerical simulation results. Figure 3 shows the experimental results compared with those of the numerical simulation. Maneuver time t_f and N in the numerical simulation are set to 5 s and 7 s, respectively. Optimal torque-shaping coefficients in Eq. (4) are listed in Table 3. Because the mathematical model is

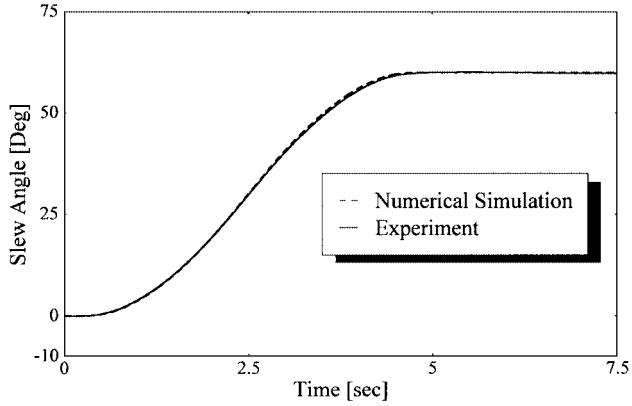

a) Slew angle

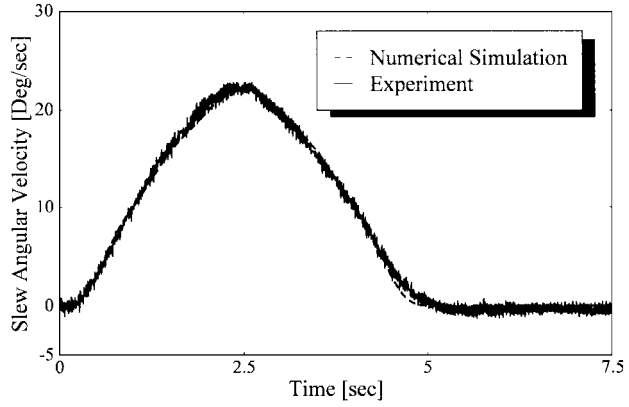

b) Slew angular velocity

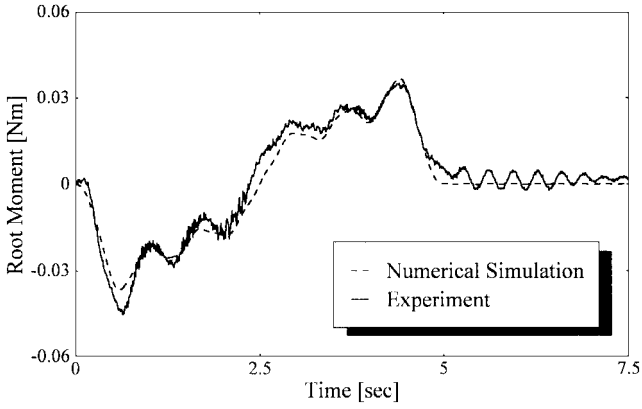

c) Root moment

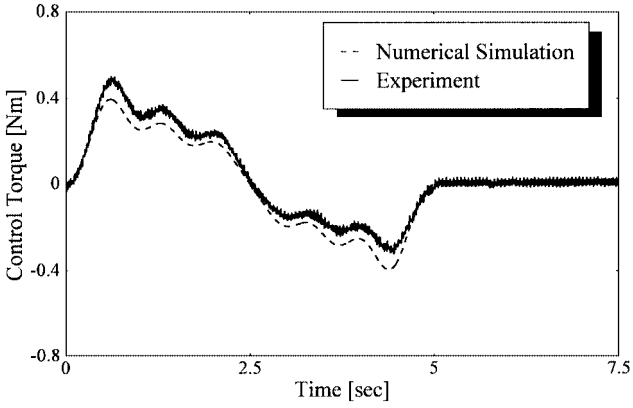

d) Hub control torque

Fig. 3 Comparative results for open-loop control law.

Table 3 Coefficients for the shaped torque

i	1	2	3	4	5	6	7
a_i	0.3164	0.0668	0.0655	−0.0051	−0.0005	−0.0362	−0.0313

modified via the identification process, these simulated results are very consistent with the experimental results. We can conclude that the experimental environment using the various compensating factors emulates the numerical model closely, and numerical analyses using the identified model guarantee that they reflect the real world.

On the other hand, an appropriate factor should be added or subtracted for each interval to take the friction torque into consideration. Motor control torque can be expressed as follows, introducing the friction factors κ and ε:

$$V(t) = \begin{cases} T_\tau^V u_r(t)(1+\kappa) & \text{for} \quad 0 \le t < t_f/2 \\ T_\tau^V u_r(t)(1-\kappa) & \text{for} \quad t_f/2 \le t < t_f \\ \varepsilon > 0 & \text{for} \quad t > t_f \end{cases} \tag{11}$$

where $V(t)$, T_τ^V, and ε are the torque command voltage applied to the motor, a conversion factor to transform the torque into the command voltage, and the command voltage negating the motor bearing friction so that the wheel speed may be kept constant after the maneuver, respectively.

Figure 4 shows the comparative results for the three open-loop control laws with respect to the slew angle measured by the encoder and the root moment measured by the piezoelectric sensor. Slew angle follows the reference maneuver well for each control law. However, the root moment history determines the performance of the adopted control methods. As is forecasted, the bang-bang control bears relatively large flexible deformation. The residual vibration for the bang-bang maneuver is expressed analytically as follows:

$$\frac{1}{2}\sum_n \left(\dot{\eta}_n^2 + \omega_n^2 \eta_n^2\right) = \sum_n 2\left[\psi_n \frac{4J_{\text{tot}}\Theta_f}{t_f^2}\left(1 - \sin\frac{\omega_n t_f}{2}\right)\right]^2 \tag{12}$$

As can be seen in Eq. (12), the residual vibration energy depends on the target angle as well as the maneuver time. Especially, the maneuver time combined with the natural frequencies of the flexible mode has a dominant effect on residual vibration. Therefore, we can control the phase of the flexible mode by changing the maneuver time. A detailed analysis and results on this observation are explained in Ref. 6. The near-minimum-time maneuver has the advantage of small and relatively flat flexible deformation during the maneuver. The shaped torque maneuver based on the trigonometric series expansion shows that the maximum root moment is higher, but lower for almost all of the maneuver interval, than the case of the near-minimum-time control. Other than the bang-bang and near-minimum-time maneuvers, the optimal coefficients for the proposed torque-shaping method are selected at every slew angle and/or the maneuver time so that the residual vibration may be sufficiently small. As a result, the residual vibration is minimized to the extent possible. Although numerical simulation perfectly eliminated the residual vibration, the experimental structure still has some friction, which has not yet been analyzed. This residual corresponds to approximately 1 $\mu\varepsilon$. Note that the residual vibration using the near-minimum-time control is almost four times that of the torque-shaping method in this particular case.

It may not be fair to compare between the bang-bang control law and the torque-shaping method directly because the torque magnitude of the torque-shaping method exceeds that of the bang-bang approach. The objective of the torque-shaping method is to design a near-minimum-time type control law while minimizing the vibration energy during and after the maneuver. If the bang-bang control law uses the maximum torque magnitude of the torque-shaping method, then the mission time of the slew maneuver would be reduced further; however, the residual vibration still exists after the mission.

B. Closed-Loop Control Experiment

The Lyapunov tracking controller is developed to follow the well-defined reference maneuver resulting in a globally stabilizing

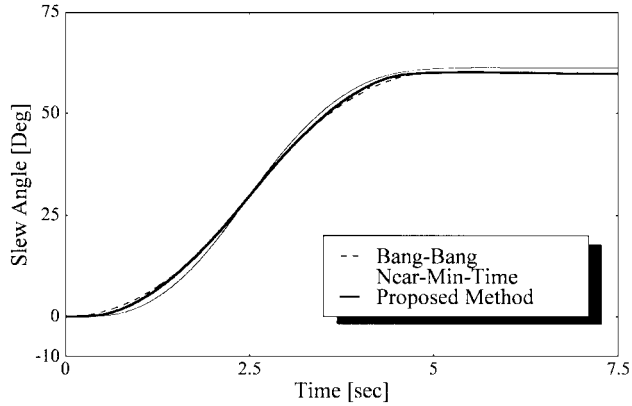

a) Slew angle

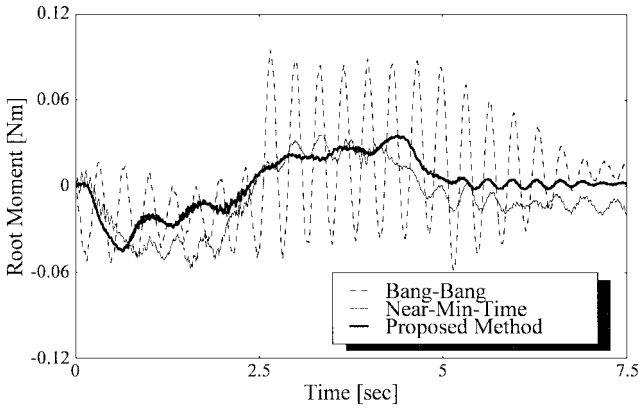

b) Root moment

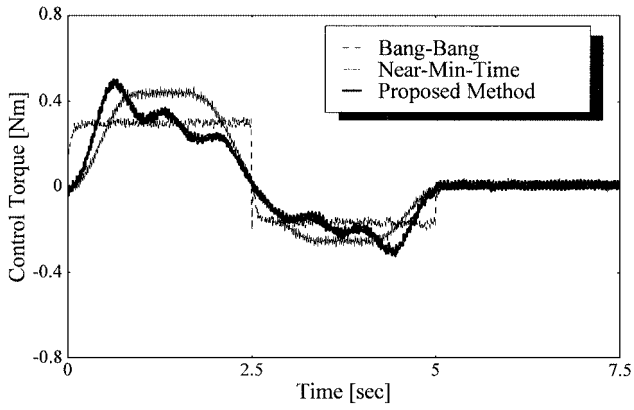

c) Hub control torque

Fig. 4 Results for various open-loop control laws.

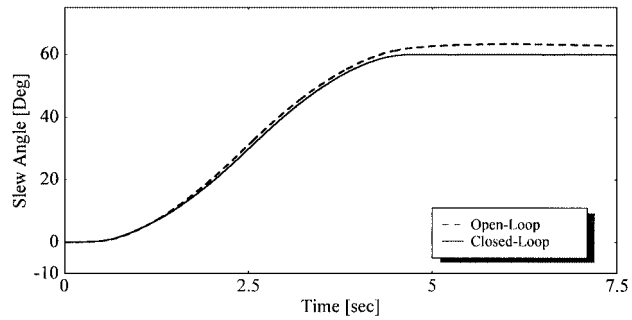

a) Slew angle

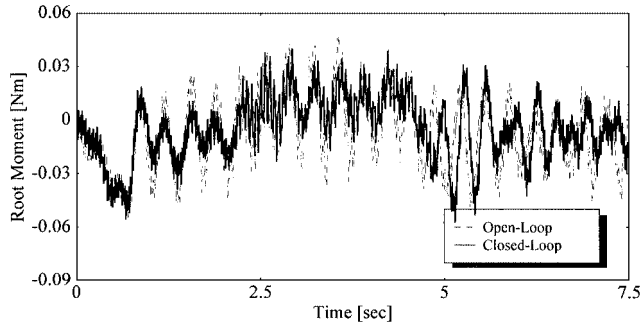

b) Root moment

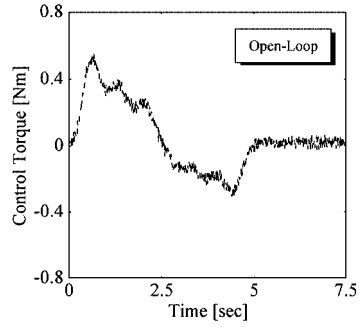

c) Open-loop control torque

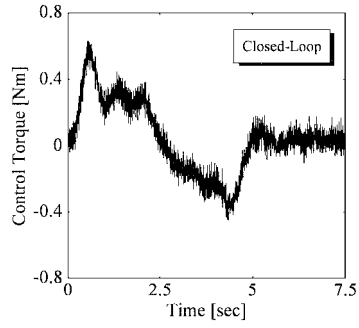

d) Closed-loop control torque

Fig. 5 Closed-loop vs open-loop control responses.

control law. The control law using optimized shaped torque input usually yields good performance for the system without external disturbance. However, a closed-loop control law should be included to guarantee the performance of slewing and vibration suppression in the presence of significant external disturbance. In this section, an optimal tracking controller is designed based on Lyapunov stability theory to follow the reference maneuver as well as to suppress inherent vibration caused by the motion of central hub.

Using the optimal torque-shaping method, the reference maneuver of FSST/SNU is designed as follows:

$$J_{\text{tot}}\ddot{\Theta}_{\text{ref}}(t) = u_{\text{ref}}(t) \tag{13}$$

where $\ddot{\Theta}_{\text{ref}}$ denotes the reference angular acceleration of the structure when the optimized torque u_{ref} is applied. Note that the commanded shaped torque generated, based on Eq. (4), is shown in Fig. 3d.

The following error energy Lyapunov function is selected to design the globally stable tracking controller considering the tracking error energy and vibration energy of the whole system[4]:

$$2U = a_1 J_h \delta\dot{\Theta}^2 + a_2 \delta\Theta^2 + 4a_3\left[\int_{l_0}^{l} \rho(\delta\dot{w} + x\delta\dot{\Theta})^2\,\mathrm{d}x + \int_{l_0}^{l} EI(\delta w'')^2\,\mathrm{d}x\right] \tag{14}$$

Using Eq. (14), the Lyapunov control law can be obtained as follows:

$$u_r(t) = u_{\text{ref}}(t) - g_1(\Theta - \Theta_{\text{ref}}) - g_2(\dot{\Theta} - \dot{\Theta}_{\text{ref}}) - g_3\left\{\int_{l_0}^{l}\left[\rho x(\ddot{w} + x\ddot{\Theta}) - \rho x^2\ddot{\Theta}_{\text{ref}}\right]\mathrm{d}x\right\} \tag{15}$$

The performance of the designed closed-loop control law is experimentally verified. The control law feeds back the slew angle, slew angular velocity, and the root moment as shown in Eq. (15). Figure 5 shows the results for the closed-loop control compared with the open-loop control where a quasirandom (0-mean, 0.0214-σ) disturbance is applied to the reaction wheel actuating. The control gains are set to be $g_1 = 30.0$, $g_2 = 5.0$, and $g_3 = 2.0$, respectively. Equation (15) illuminates that the adopted Lyapunov control law takes the form of output feedback control in the sense that all of the feedback terms are measured using individual sensors. The overall control update frequency is set to be 100 Hz. As can be seen in Figs. 3 and 4, well-modeled friction compensation strategy enables the open-loop system to exhibit good performance. However, the open-loop control law cannot guarantee the same performance in the presence of the external disturbance and/or variation of the other peripheral environments. Figure 5 shows the better performance of the closed-loop control methodology than the open-loop control. Despite the disturbance, the tracking controller achieves accurate targeting while suppressing flexible deformation. Note that relatively large control gains increase the control input and may destabilize the system in the presence of the various sources of disturbance. The desired objectives of targeting and vibration control can be met by assigning appropriate control gains.

V. Conclusion

In this paper, the performance of the proposed torque-shaping method is verified by a systematic experimental procedure. FSST/SNU dynamic modeling is identified so that the mathematical model can reflect the real structure. As a consequence, the results of the numerical simulation mirror the experimental duplicates by showing almost the same responses. Compared with the bang-bang maneuver and the near-minimum-time maneuver, the proposed torque-shaping method proved to have better performance in view of residual vibration. Also, the closed-loop experiment shows successful precise targeting irrespective of the various external disturbances by adopting the tracking controller.

Acknowledgment

This research was supported by the Korea Aerospace Research Institute, Contract KOMPSAT System Design and Development (IV).

References

[1] Liu, Q., and Wie, B., "Robust Time-Optimal Control of Uncertain Flexible Spacecraft," *Journal of Guidance, Control, and Dynamics*, Vol. 15, No. 3, 1992, pp. 597–604.

[2] Singh, T., and Vadali, S. R., "Robust Time-Optimal Control: A Frequency Domain Approach," *Journal of Guidance, Control, and Dynamics*, Vol. 17, No. 2, 1994, pp. 346–353.

[3] Singhose, W., Banerjee, A., and Seering, W., "Slewing Flexible Spacecraft with Deflection-Limiting Input Shaping," *Journal of Guidance, Control, and Dynamics*, Vol. 20, No. 2, 1997, pp. 291–298.

[4] Junkins, J. L., Rahman, Z., and Bang, H., "Near-Minimum Time Control of Distributed Parameter Systems: Analytical and Experimental Results," *Journal of Guidance, Control, and Dynamics*, Vol. 14, No. 2, 1991, pp. 406–415.

[5] Aspinwall, D. M., "Acceleration Profiles for Minimizing Residual Response," *Journal of Dynamic Systems, Measurement, and Control*, Vol. 112, No. 1, 1990, pp. 3–6.

[6] Suk, J., Moon, J., and Kim, Y., "Torque Shaping Using Trigonometric Series Expansion for Slewing of Flexible Structures," *Journal of Guidance, Control, and Dynamics*, Vol. 21, No. 5, 1998.

[7] Junkins, J. L., and Kim, Y., *Introduction to Dynamics and Control of Flexible Structures*, AIAA Education Series, AIAA, Washington, DC, 1993, Chap. 4.

[8] Junkins, J. L., and Turner, J. D., *Optimal Spacecraft Rotational Maneuvers*, Elsevier, Amsterdam, 1986, Chap. 6.